Journal of Thermal Analysis and Calorimetry (2019) 136:885–892
https://doi.org/10.1007/s10973-018-7687-8

# Thermodynamic study of direct reduction of high-chromium vanadium–titanium magnetite (HCVTM) based on phase equilibrium calculation model

Mi Zhou[1,2] · Tao Jiang[1,2] · Xueyong Ding[1] · Shihong Ma[1] · Guo Wei[1] · Xiangxin Xue[1,2]

Received: 20 April 2018 / Accepted: 17 August 2018 / Published online: 3 September 2018


**Abstract**
High-chromium vanadium–titanium magnetite (HCVTM) is a good valuable resource with high iron content in the form of complex iron ore which contains various valuable metal elements such as iron, vanadium, titanium, chromium. Direct reduction of HCVTM is studied based on thermodynamic analysis. Combined TG experimental verification and equilibrium calculation model was used to analyze the reaction sequence and equilibrium amount in this paper. The contents in HCVTM reduction system are simplified as 18 kinds of chemical compositions. Reductions of $Fe_3O_4$ and $FeO{\cdot}TiO_2$ are the main reduction reactions and are mainly reduced by C. The reduction reaction sequence of $FeO{\cdot}TiO_2$ is $FeO{\cdot}TiO_2$, $TiO_2$, TiC, and Ti; the reduction reaction sequence of $Fe_3O_4$ is $Fe_3O_4$, FeO, and Fe. The minimum reduction temperature of HCVTM is 860 °C. The reduction of Cr is difficult to implement, and the minimum reduction temperature of V is above 700 °C. The gas phase in this system is mainly CO when the temperature is above 1000 °C. CO partial pressure curve of gasification reaction is in the shape of 'S' with increase of temperature. When the temperature is 1350 °C, C/O is 1.0 and reduction time is 30 min, HCVTM can be reduced thoroughly and the reduction degree can reach to 0.98. When C/O is lower than 1.0, $FeTi_2O_5$ is the reduction intermediate products from $FeO{\cdot}TiO_2$. When C/O is 1.0, diffraction peaks of $Fe_3O_4$ and $FeO{\cdot}TiO_2$ disappear, and they are reduced to Fe and $TiO_2$.

**Keywords** Phase equilibrium · Thermodynamic analysis · Reduction · High-chromium vanadium–titanium magnetite · Thermodynamic analysis

## Introduction

High-chromium vanadium–titanium magnetite (HCVTM) is a typically complex polymetallic iron ore resource with abundant reserves in China, Russia, North Africa, and America [1, 2]. It is mainly deposited in Panxi area in the Sichuan province, China, and has a high comprehensive utilization value [3]. Iron (Fe), vanadium (V), titanium (Ti), and chromium (Cr), which are contained in HCVTM, are recognized important strategic resources all over the world. The form of iron in HCVTM is in complex phase which contains various valuable metal elements such as Fe, V, Ti, and Cr [4]. The main phase in HCVTM is magnetite ($Fe_3O_4$), ilmenite ($FeTiO_3$), and chromite ($FeCr_2O_4$). V in HCVTM is mainly in the phase of $FeV_2O_4$ [2]. HCVTM is a good valuable resource with high iron content.

At present, the iron production from HCVTM in blast furnace is common method. However, it is difficult to make blocks and smelt in blast furnace for this complex composition. Therefore, it decreases the utilization of Fe, V, Ti, and Cr in HCVTM comprehensively. However, the Fe, V, and Ti recovery ratio are only about 70, 39, and 13%, respectively [2, 5]. Besides, the insufficient recovery of valuable metals leads to serious resource waste and environment pollution [6, 7]. Due to the dispersed distribution of Ti components in various fine grained ($< 10$ μm)

✉ Mi Zhou
zhoum@smm.neu.edu.cn

[1] School of Metallurgy, Northeastern University, NO 11, Lane 3, Wenhua Road, Heping District, P.O. Box 345, Shenyang 110819, Liaoning, People's Republic of China

[2] Key Laboratory of Liaoning Province for Recycling Science of Metallurgical Resources, Shenyang 110819, People's Republic of China

mineral phases with complex interfacial combination, it is difficult to recover Ti components and metallic iron through traditional separation processes [7].

In order to achieve the efficient separation and comprehensive utilization of Fe, V, Ti, Cr, and other resources, some attempts have been carried out. Lv [5] studied reduction of vanadium titanomagnetite by microwave irradiation method and the recovery of iron reached 60%. The iron recovery cannot increase further. Zhang [8] proposed pressure leaching method to recover iron from vanadium slag with waste titanium dioxide. V and Fe leaching ratios are 93.50% and 96.85%, respectively. However, energy consumption and operational complexity limit the development of this method. The recoveries will bring some difficulties to subsequent hydrometallurgy extraction. This can be used for the smelting of vanadium–titanium magnetite concentrate without using coke or coal.

High-grade sponge iron obtained by direct reduction–melting of HCVTM can be used as a raw material for electric furnace steelmaking instead of scrap steel, achieving the preliminary separation of iron, chromium, vanadium and titanium, and laying the foundation for subsequent comprehensive utilization. In particular, coal-based direct reduction–melting processes have gradually developed into an alternative technology for processing vanadium–titanium magnetite concentrates [6, 9–12]. In Chen's [6] experiment, the process of metalizing reduction and magnetic separation for vanadium titanomagnetite (enriched in the titanium-bearing slag) was proposed. The recovery ratios of Fe, V, and Ti are 91.19, 61.82, and 85.31%, respectively. Yuan [9] proposed a new process, in which Panzhihua ilmenite concentrate was first reduced in a rotated hearth furnace to produce iron and titanium-enriched material, and then the latter was chloridized in a new combined fluidized bed to produce $TiCl_4$. With pulverized coal, titanomagnetite concentrates was reduced in Chen's [10] experiment. The metallization degree of pre-oxidized titanomagnetite concentrates reached 96.4%, after heating for 1 h at 1200 °C. Upgrading metal's by direct reduction from HCVTM was studied by Saikat [11]. Fe/$TiO_2$ was upgraded about to 7.06 in the magnetic fraction of reduced lump ore which was formerly 2.14. In Zhao's research [12], most of V, Cr, and Ti were concentrated into slag by the process of coal-based reduction–magnetic separation for HCVTM. The recoveries of V, Cr, and Ti are only about 40, 80, and 20%, respectively. However, basic research of reactions in this process is still weak. Further in-depth study of the direct reduction behavior of vanadium–titanium magnetite is significant for the improvement in the technology and industrial application.

Based on the circumstance of the HCVTM, it is necessary to strengthen the reduction vanadium titanium magnetite. Thermodynamic studies on the standard Gibbs free energy changes ($\Delta G^{\theta}$) and have been applied for feasibility analysis before practical experiments [13–17]. Some key reactions were carried out by this method [18, 19]. Owing to the complex compositions of HCVTM, the reactions involved in the reduction process are complicated. Therefore, thermodynamic results obtained by $\Delta G^{\theta}$ may not be representative of the real process. Besides, the formation of iron containing phase is difficult to investigate by key reactions.

To establish internal reduction reaction mechanism and make clear the transformation behavior of the species in this system, the main components of HCVTM are taken into account. Based on Gibbs free energy principle and Phase Equilibrium Calculating Model in HSC Chemistry software, the detailed thermodynamic study was performed. By comparison, feasibility experiments of the direct reduction were carried out. Recovery ratio and XRD patterns of the reduced HCVTM was studied.

## Materials and methods

### Material

In this paper, HCVTM was supplied from Panzhihua City, China. Its chemical composition in this paper is shown in Table 1. The phases of raw materials were identified by X-ray diffractometer (XRD). Figure 1 presents XRD patterns of it before the reduction reaction. Figure 1 indicates that the main phases in HCVTM are magnetite ($Fe_3O_4$), ilmenite ($FeTiO_3$), and chromite ($FeCr_2O_4$). The contents in HCVTM reduction system are simplified as Fe, $Fe_3O_4$, FeO, CaO, $CaCO_3$, MgO, $SiO_2$, $Al_2O_3$, Ti, TiC, $TiO_2$, Cr, $Cr_2O_3$, V, $V_2O_5$, C, CO, $CO_2$, 18 kinds of chemical compositions.

### Methods

The equilibrium compositions were calculated by Phase Equilibrium Calculating Model of HSC Chemistry based on the minimization of the total Gibbs free energy. And the

**Table 1** Chemical composition of high-chromium vanadium–titanium magnetite (HCVTM) concentrate (mass%)

| Composition | TFe | FeO | $TiO_2$ | $SiO_2$ | $Al_2O_3$ | MgO | CaO | $V_2O_5$ | $Cr_2O_3$ | P | S |
|---|---|---|---|---|---|---|---|---|---|---|---|
| Content | 50.16 | 26.47 | 12.44 | 4.60 | 2.58 | 3.68 | 0.48 | 0.57 | 1.28 | < 0.01 | 0.15 |

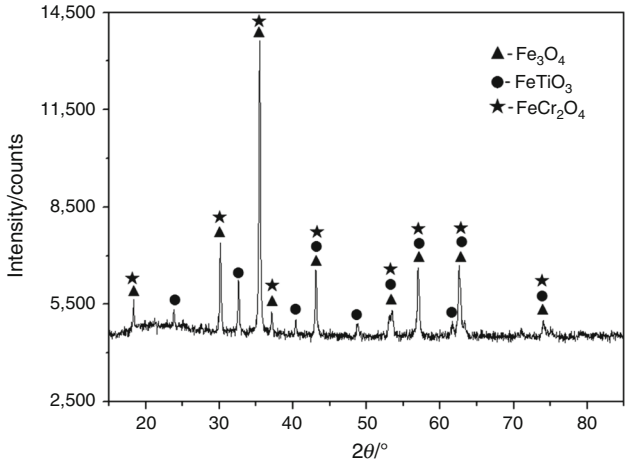


**Fig. 1** XRD pattern of HCVTM concentrate

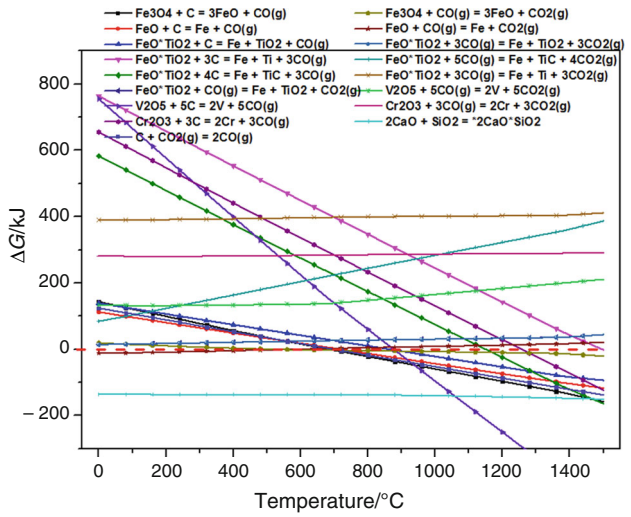


**Fig. 2** Free Gibbs energy change of reactions in HCVTM reduction system

amount of the main contents was calculated by molar weight. The initial HCVTM amount data and addition of reducer are shown in Table 2. The reducer addition ratio of C/O is 1.0. The theoretical molar quantity of 'O' in FeO and $Fe_3O_4$ is 213.18 mol. And the addition reducer molar quantity of C is 213.18 mol. The thermodynamic analysis is conducted taking the following assumed conditions into account:

(1) The mass of HCVTM ore is 100 kg.
(2) Atmosphere pressure of calculation system is 0.1 MPa.
(3) In this paper, contents lower than 0.5% are not discussed.
(4) The unstable phase composition formed in reaction system is not considered.
(5) The reducer is simplified as molding compound C.
(6) Direct and indirect reduction reactions take place at the same time. The reduction reactions and equilibrium compositions are discussed.

## Results and discussion

### Thermodynamic analysis of reduction reactions in HCVTM

Reactions of HCVTM reaction system include direct reductions reactions of C [Eqs. (1)–(7)], indirect reduction reactions of CO [Eqs. (8)–(14)], gasification reactions [Eq. (14)], slagging reaction [Eq. (15)]. The reduction reactions in HCVTM contains reduction of FeO, $Fe_3O_4$, $FeO{\cdot}TiO_2$, $V_2O_5$, and $Cr_2O_3$ by C and CO. Based on the chemical composition of HCVTM as shown in Table 1. Contents of CaO and $SiO_2$ are 0.48% and 4.60%, respectively. Mole ratio of CaO and $SiO_2$ is much lower than 1.0, which means that CaO is insufficient to produce $2CaO{\cdot}SiO_2$, $3CaO{\cdot}SiO_2$ with $SiO_2$. In other words, $CaO{\cdot}SiO_2$ is produced merely.

Based on Gibbs principle of the minimization of the total Gibbs free energy, the reaction can proceed spontaneously when the Gibbs free energy change is lower than zero. Figure 2 shows the Gibbs free energy change curves of reactions with the change of temperature. For most reactions, Gibbs free energy decreases to lower than zero with the increase in temperature. With the increase in temperature, the Gibbs free energy of reduction reactions of $FeO{\cdot}TiO_2$, $Cr_2O_3$ by CO remained steady. However, the reduction of $FeO{\cdot}TiO_2$, $V_2O_5$, and $Cr_2O_3$ by CO could not proceed spontaneously. Besides, production reactions of Fe and Ti from $FeO{\cdot}TiO_2$ is strict and the temperature of should be above than 1490 °C.

Equations (3)–(5) produce different states of Ti element. Compared with Eqs. (3), (4), and (5), $FeO{\cdot}TiO_2$ will convert to Fe and $TiO_2$ easier by Gibbs free energy results. From Fig. 2, Gibbs free energy of Eqs. (3)–(5) are in the sequence of $TiO_2$, TiC and Ti. In other words, $FeO{\cdot}TiO_2$ reduction by C is in the sequence of $FeO{\cdot}TiO_2$, $TiO_2$, TiC,

**Table 2** Proximate analysis of coal and chemical composition of ash in coal (mass%)

| Fixed carbon | Volatile | Moisture | S | P | Ash | | | | |
|---|---|---|---|---|---|---|---|---|---|
| | | | | | FeO | CaO | MgO | $SiO_2$ | $Al_2O_3$ |
| 78.62 | 6.80 | 2.74 | 0.67 | 0.04 | 0.56 | 0.37 | 0.15 | 5.97 | 4.08 |

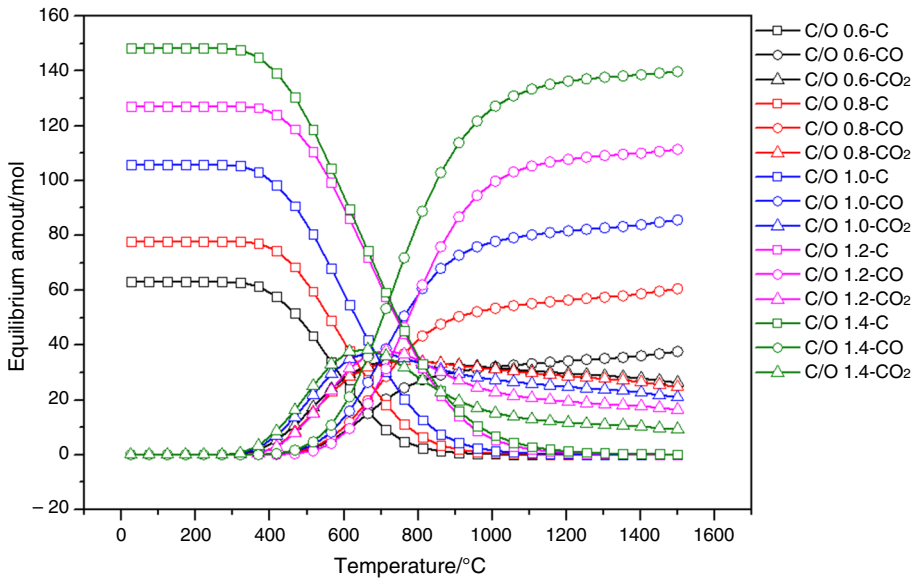


**Fig. 3** Equilibrium amount of gas phase

and Ti. When the FeO is separated from $FeO{\cdot}TiO_2$, the reduction of FeO will be reduced by C, which is shown in Fig. 2. Slagging reaction and gasification reaction can react spontaneously.

$$Fe_3O_4 + C = 3FeO + CO(g) \quad (1)$$

$$FeO + C = Fe + CO(g) \quad (2)$$

$$FeO{\cdot}TiO_2 + C = Fe + TiO_2 + CO(g) \quad (3)$$

$$FeO{\cdot}TiO_2 + 4C = Fe + TiC + 3CO(g) \quad (4)$$

$$FeO{\cdot}TiO_2 + 3C = Fe + Ti + 3CO(g) \quad (5)$$

$$V_2O_5 + 5C = 2V + 5CO(g) \quad (6)$$

$$Cr_2O_3 + 3C = 2Cr + 3CO(g) \quad (7)$$

$$Fe_3O_4 + CO(g) = 3FeO + CO_2(g) \quad (8)$$

$$FeO + CO(g) = Fe + CO_2(g) \quad (9)$$

$$FeO{\cdot}TiO_2 + CO(g) = Fe + TiO_2 + CO_2(g) \quad (10)$$

$$FeO{\cdot}TiO_2 + 4CO(g) = Fe + TiC + 3CO_2(g) \quad (11)$$

$$FeO{\cdot}TiO_2 + 3CO(g) = Fe + Ti + 3CO_2(g) \quad (12)$$

$$V_2O_5 + 5CO(g) = 2V + 5CO_2(g) \quad (13)$$

$$Cr_2O_3 + 3CO(g) = 2Cr + 3CO_2(g) \quad (14)$$

$$C + CO_2(g) = 2CO(g) \quad (15)$$

$$2CaO + SiO_2 = 2CaO{\cdot}SiO_2 \quad (16)$$

## Effects of C/O and temperature on equilibrium amount

Effects of C/O on equilibrium amount and enthalpy are shown in Figs. 3, 4, and 5. Equilibrium amount of gas phase is shown in Fig. 3. With the increase in C/O,

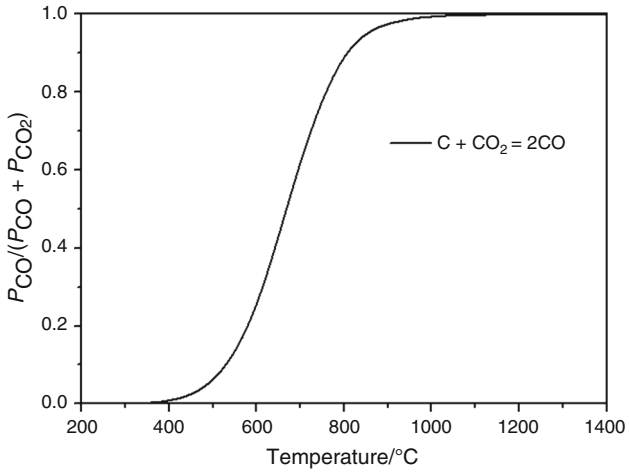


**Fig. 4** Equilibrium curve of carbon gasification

equilibrium amounts of C and CO increase gradually and equilibrium amount of $CO_2$ declines steadily. This is because that excess C promotes reduction reactions of C [Eqs. (1)–(7)] move forward and weakens the reduction reactions of CO [Eqs. (8)–(14)].

With the increase in temperature, equilibrium amount of C decreases gradually and equilibrium amount of CO increases gradually at the same conversion temperature region as C. The consumption of C mainly turns into CO. Besides, the equilibrium amount of $CO_2$ reaches a peak obviously at about 700 °C. When the temperature is higher than 700 °C, equilibrium amount decreases slowly. The gas phase in this system is mainly CO when the temperature is above 1000 °C. This is because that gasification reaction takes place in the system. As shown in Fig. 4, CO partial pressure curve of gasification reaction is in the shape of 'S' with increase in temperature.

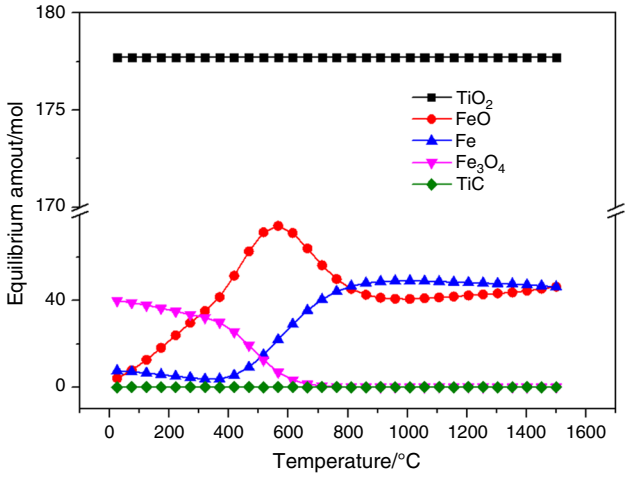


**Fig. 5** Equilibrium amount of Fe and Ti phase

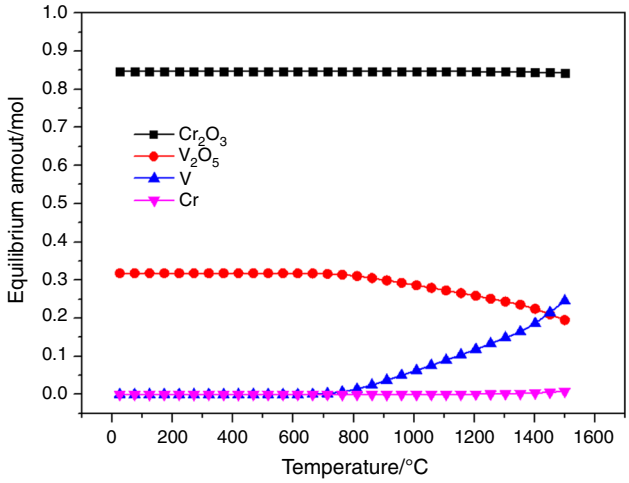


**Fig. 6** Equilibrium amount of Cr and V phase

Equilibrium amount curves of Fe and Ti element phases are shown in Fig. 5. Equilibrium amount of $TiO_2$ and TiC remain steady. The equilibrium amount of TiC is close to zero. Phase equilibrium calculation results of $TiO_2$ and TiC are in accordance with Free Gibbs Energy Change analysis results.

The equilibrium amount of FeO reaches a peak at 566 °C and then suddenly drops to 40 mol and finally remains steady above 860 °C. Equilibrium amount of Fe increases dramatically and remains steady above 860 °C. Equilibrium amount of $Fe_3O_4$ decreases gradually and remains close to zero steadily above 860 °C. In other words, the minimum reduction temperature of HCVTM should be above 860 °C.

Equilibrium amount curves of Cr and V phase are shown in Fig. 6. The amount of Cr and $Cr_2O_3$ is steady. As analyzed by Gibbs free energy calculation results in Fig. 2, the reduction of Cr is difficult to implement. When temperature is above 700 °C, equilibrium amount of V increases gradually and equilibrium amount $V_2O_5$ drops gradually. In other words, the minimum reduction temperature of V is above 700 °C.

## Effects of C/O and temperature on theoretical reduction degree and enthalpy

To make sure the reduction degree theoretically, theoretical reduction degree is determined as follow [19]:

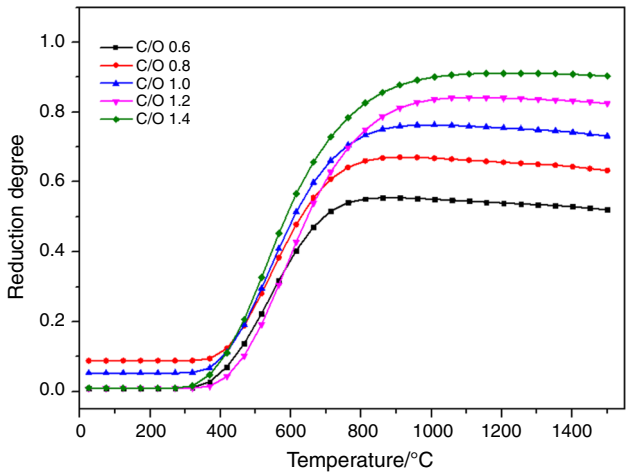


**Fig. 7** Effects of C/O on reduction degree theoretically

where $n_0$ (FeO), $n_0$ ($Fe_3O_4$), and $n_0$ ($TiO_2$) are molar quantity of FeO, $Fe_3O_4$, and $TiO_2$ in iron ore before reduction, respectively, $n_1$ (FeO), $n_1$ ($Fe_3O_4$), and $n_1$ ($TiO_2$) are molar quantity of FeO, $Fe_3O_4$, and $TiO_2$ in iron ore after reduction, respectively. Because the main $TiO_2$ reduction production of HCVTM is TiC, every mole of $TiO_2$ will consume 3 mol of C. Thus, the coefficient of $TiO_2$ in Eq. (17) is three. The C consumption of $V_2O_5$ and $Cr_2O_3$ reduction is neglected.

Effects of C/O on HCVTM theoretical reduction degree curves by phase equilibrium calculation are shown in Fig. 7. With the increase of C/O, theoretical reduction

$$\eta = \frac{n_0(\mathrm{FeO}) + 4 \times n_0(\mathrm{Fe_3O_4}) + 3 \times n_0(\mathrm{TiO_2}) - n_1(\mathrm{FeO}) - 4 \times n_1(\mathrm{Fe_3O_4}) - 3 \times n_1(\mathrm{TiO_2})}{n_0(\mathrm{FeO}) + 4 \times n_0(\mathrm{Fe_3O_4}) + 3 \times n_0(\mathrm{TiO_2})} \quad (17)$$

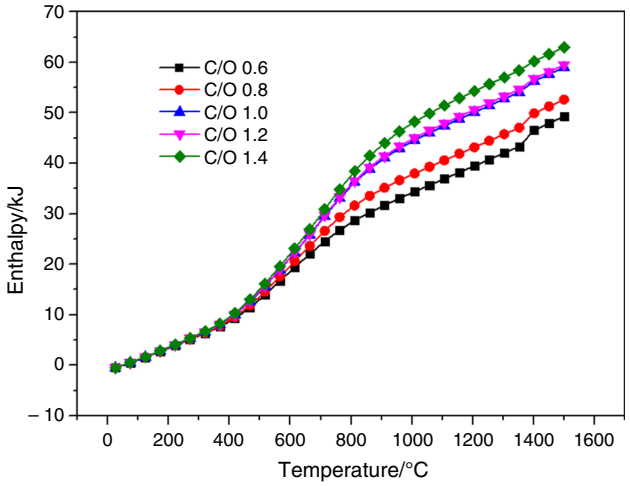


**Fig. 8** Effects of C/O on chemical reaction system enthalpy

degree increased gradually. For different C/O ratio, reduction temperature region is same. The initial temperature of HCVTM is about 380 °C. And when the temperature is above 1000 °C, the reduction degree curve remain steady.

Enthalpy of chemical reaction curves in system is shown in Fig. 8. With the increase of temperature, enthalpy increased gradually. And with the addition of C, enthalpy in system is improved.

## Reduction characteristics of HCVTM by TG–DSC

To investigate the direct reduction feasibility of HCVTM, reduction experiments were carried out, using NETZSCH STA 409 C/CD comprehensive thermal analyzer. The sample is mixture of coal and HCVTM by different C/O. The diameter of coal and HCVTM is smaller than 250 μm. The chemical contents of coal are shown in Table 2. In each experiment, about 10 mg of samples were heated at heating rate of 10 °C $min^{-1}$ in $N_2$ atmosphere.

In heating process, TG–DSC curves of the mixture of HCVTM and coal are shown in Fig. 9. The mixture has three reduction mass loss temperature regions. The temperature is at 644–985 °C. DSC curve has an endothermic peak. In this region, the reduction reaction of $Fe_3O_4$ takes place. When the temperature is at 985–1160 °C, the drastic mass loss appears. In this region, some reduction reactions of $FeO{\cdot}TiO_2$ takes place. When the temperature is at 1160–1400 °C, several DSC endothermic peaks appear. Deoxygenations of $Cr_2O_3$, $V_2O_3$ and $TiO_2$ take place.

By thermal weightlessness method, reduction degree of HCVTM is calculated at 1200 °C, 1250 °C, 1300 °C and 1350 °C. In this experiment, all data were acquired in isothermal reduction conditions. Based on the analysis of mass loss of samples in TG curves, reduction degree was calculated. The reduction degree $R$ is defined as the following formula:

$$R_{\mathrm{t}} = \frac{\Delta m_{\mathrm{O}}^{\mathrm{t}}}{\Delta m_{\mathrm{O}}^{0}} \tag{18}$$

$R_t$ is reduction degree at time $t$, $s$; $\Delta m_{\mathrm{O}}^{\mathrm{t}}$ is the mass loss of oxygen at time $t$, $g$; $\Delta m_{\mathrm{O}}^{0}$ is the total mass of oxygen in HCVTM and $\Delta m_{\mathrm{O}}^{0}$ is 0.18557 $m_0$ in this experimental samples, $g$; $m_0$ is the initial mass of HCVTM, $g$.

The mass loss of reduction oxygen and fixed carbon from coal can be calculated by the formula as follow:

$$\Delta m_{\mathrm{t}} = \Delta m_{\Sigma}^{\mathrm{t}} - \Delta m_{\mathrm{V}}^{\mathrm{t}} - \Delta m_{\mathrm{M}}^{\mathrm{t}} \tag{19}$$

where $\Delta m_{\mathrm{t}}$ the mass loss of reduction oxygen and fixed carbon at time $t$, $g$; $\Delta m_{\Sigma}^{\mathrm{t}}$ is total mass loss of sample mixture at time $t$, $g$; $\Delta m_{\mathrm{V}}^{\mathrm{t}}$ is the mass loss of volatiles and water at time $t$, $g$; $\Delta m_{\mathrm{M}}^{\mathrm{t}}$ is mass loss of heating process of iron ore, $g$.

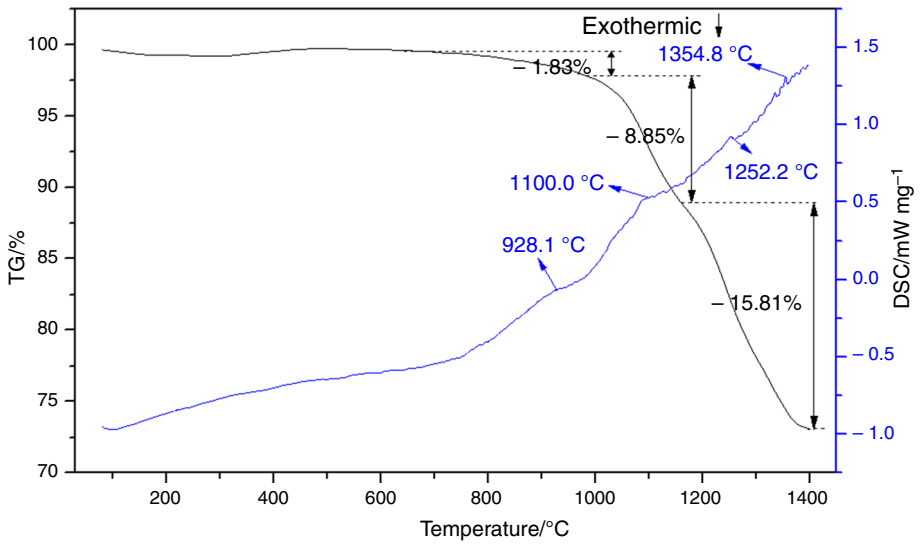


**Fig. 9** TG–DSC curves of the mixture of HCVTM and coal

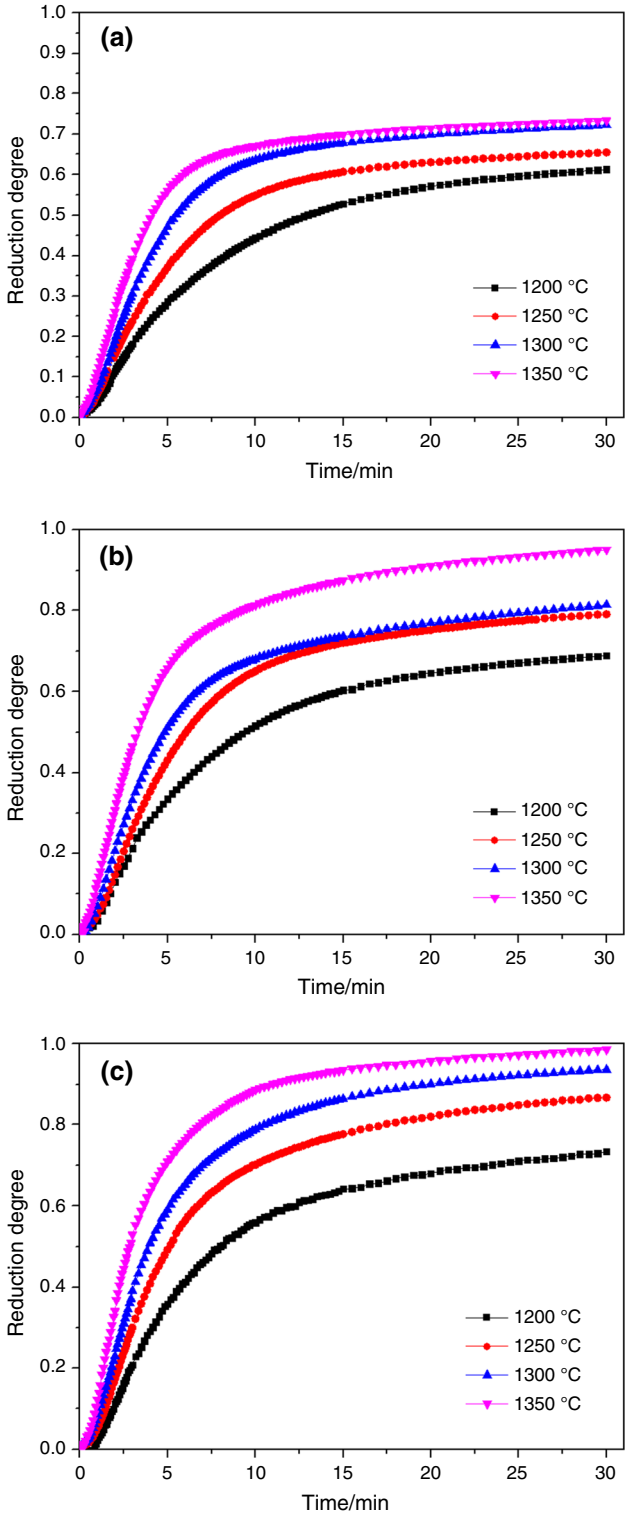


**Fig. 10** Reduction degree of HCVTM by different C/O. **a** C/O = 0.6; **b** C/O = 1.0, **c** C/O = 1.4

Analyzed by gasification curve of C gasification, when the temperature is higher than 1100 °C, partial pressure of CO is nearly to 1. Thus, the direct reduction by CO can be

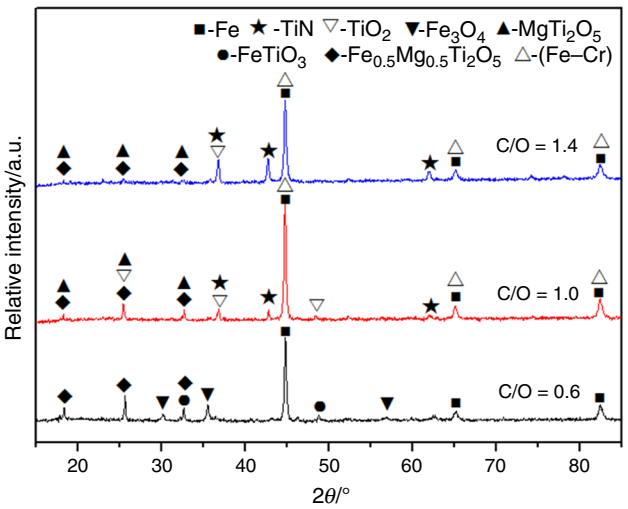


**Fig. 11** XRD patterns of reduction products at different C/O (temperature: 1350 °C, reduction time: 30 min)

neglected when the temperature is higher than 1100 °C. In the reduction process, reduction oxygen and fixed carbon all outflow in the form of CO. Thus, the reduction oxygen mass loss at time t is as follows:

$$\Delta m_{\mathrm{O}}^{\mathrm{t}} = \frac{16}{28}\Delta m_{\mathrm{t}} \tag{20}$$

Samples are heated at programmed temperatures (1200 °C, 1250 °C, 1300 °C and 1350 °C) respectively with heating rate of 10 °C $\mathrm{min}^{-1}$. Then we kept the temperature constant for 30 min. Finally, the samples were cooled in reactor with $N_2$. The reactor temperature of was measured by thermocouples of type *K* through the measuring point and the temperature measurement error is below 0.5 °C.

Reduction degree of HCVTM is shown in Fig. 10, when C/O are 0.6, 1.0, and 1.4 at 1200 °C, 1250 °C, 1300 °C and 1350 °C, respectively. The tendency of sample reduction degree curves are in the same. In initial reaction region (1–5 min), reduction degree increased sharply. With the increase in time, medium reaction region (5–10 min) increase rate becomes lower. In later reaction region (10–30 min), curves level off.

With the increase in C/O, reduction degree increases obviously. And reduction degree is affected by temperature. At higher temperature, samples have larger reduction rate and higher reduction degree.

Analyzed by XRD, phases of reduction products are shown in Fig. 11. When C/O is 0.6, the main phase of products are $Fe_{0.5}Mg_{0.5}Ti_2O_5$, $Fe_3O_4$, $FeO{\cdot}TiO_2$, and Fe. Due to the lack of fixed carbon, $Fe_3O_4$ and $FeO{\cdot}TiO_2$ have not been reduced thoroughly. Besides, $FeTi_2O_5$ is the reduction intermediate products from $FeO{\cdot}TiO_2$. However,

the structure of $FeTi_2O_5$ is instable. When C/O is 1.0, diffraction peaks of $Fe_3O_4$ and $FeO{\cdot}TiO_2$ disappear, and they are reduced to Fe and $TiO_2$. And thermodynamic analysis of $FeO{\cdot}TiO_2$ reaction [Eq. (3)] can be demonstrated. In $N_2$ atmosphere, some TiN is generated as shown in Eq. (21). And some Cr moved into reduced Fe and Fe–Cr diffraction peak occurs. When C/O is 1.3, types of main phase of products does not change.

$$FeO{\cdot}TiO_2 + 3C + 1/2N_2(g) = TiN + Fe + 3CO(g) \quad (21)$$

## Conclusions

Thermogravimetric analysis of direct reduction of high-chromium vanadium–titanium magnetite (HCVTM) based on phase equilibrium calculation model and TG experiments are carried out. The conclusions are as follows.

(1) The contents in HCVTM reduction system are simplified as 18 kinds of chemical compositions. The indirect reduction of $FeO{\cdot}TiO_2$, $V_2O_5$, and $Cr_2O_3$ by CO could not proceed spontaneously. $FeO{\cdot}TiO_2$ reduction by C is in the sequence of $FeO{\cdot}TiO_2$, $TiO_2$, TiC, and Ti.

(2) When the temperature is above 1000 °C, gas phase in this system is mainly CO. CO partial pressure curve of gasification reaction is in the shape of 'S' with increase of temperature.

(3) The minimum reduction temperature of HCVTM should be above 860 °C. The reduction of Cr is difficult to implement and the minimum reduction temperature of V is above 700 °C.

(4) The reduction degree tendency of theoretical calculation results by equilibrium calculation model and experimental results are in the same. When C/O is 0.6, $Fe_3O_4$ and $FeO{\cdot}TiO_2$ have not been reduced thoroughly. When temperature is 1350 °C, C/O is 1.0 and reduction time is 30 min, HCVTM can be reduced thoroughly and the reduction degree reaches to 0.98. Besides, $FeTi_2O_5$ is instable and it the reduction intermediate products of $FeO{\cdot}TiO_2$.

**Acknowledgements** The author will acknowledge the support from National Natural Science Foundation of China (Nos. 51604065 & 51674084), the Major State Research Development Program of China (Nos. 2017YFB0603800 & 2017YFB0603804), the Fundamental Funds for the Program of the Science Foundation of Liaoning Province (No. 20170540316), the Fundamental Research Funds for the Central Universities (No. N172507012).

## References

1. Tang J, Chu MS, Ying ZW, et al. Non-isothermal gas-based direct reduction behavior of high chromium vanadium–titanium magnetite pellets and the melting separation of metallized pellets. Metals. 2017;7(5):153.
2. Tang J, Chu MS, Feng C, et al. Melting separation behavior and mechanism of high-chromium vanadium-bearing titanomagnetite metallized pellet got from gas-based direct reduction. ISIJ Int. 2016;56(2):210–9.
3. Hu ML, Liu L, Lv XW, et al. Crystallization behavior of perovskite in the synthesized high-titanium-bearing blast furnace slag using confocal scanning laser microscope. Metall Mater Trans B. 2013;45(1):76–85.
4. Long HM, Chun TJ, Wang P, et al. Grinding kinetics of vanadium–titanium magnetite concentrate in a damp mill and its properties. Metall Mater Trans B. 2016;47(3):1765–72.
5. Lv XW, Lun ZG, Yin JQ, et al. Carbothermic reduction of vanadium titanomagnetite by microwave irradiation and smelting behavior. ISIJ Int. 2013;53(7):1115–9.
6. Chen SY, Fu XJ, Chu MS, et al. Life cycle assessment of the comprehensive utilisation of vanadium titano-magnetite. J Clean Prod. 2015;101:122–8.
7. Zhang L, Zhang LN, Wang MY, et al. Recovery of titanium compounds from molten Ti-bearing blast furnace slag under the dynamic oxidation condition. Miner Eng. 2007;20(7):684–93.
8. Zhang GQ, Zhang TA, Zhang Y, et al. Pressure leaching of converter vanadium slag with waste titanium dioxide. Rare Met. 2014;35(7):576–80.
9. Yuan ZF, Wang XQ, et al. A new process for comprehensive utilization of complex titania ore. Miner Eng. 2006;19(9):975–8.
10. Chen DS, Song B, Wang LN, et al. Solid state reduction of Panzhihua titanomagnetite concentrates with pulverized coal. Miner Eng. 2011;24(8):864–9.
11. Samanta S, Mukherjee S, Dey R. Upgrading metals via direct reduction from poly-metallic titaniferous magnetite ore. JOM. 2014;67(2):467–76.
12. Zhao LS, Wang LN, Chen DS, et al. Behaviors of vanadium and chromium in coal-based direct reduction of high-chromium vanadium-bearing titanomagnetite concentrates followed by magnetic separation. T Nonferr Metal Soc. 2015;25(4):1325–33.
13. Yu W, Tang QY, Chen JA, et al. Thermodynamic analysis of the carbothermic reduction of a high-phosphorus oolitic iron ore by FactSage. Int J Miner Met Mater. 2016;23(10):1126–32.
14. He JHO, Kim BS, Park JH. Effect of CaO addition on iron recovery from copper smelting slags by solid carbon. Metall Mater Trans B. 2013;44(6):1352–63.
15. Xie HQ, Yu QB, Zuo ZL, et al. Thermodynamic analysis of hydrogen production from raw coke oven gas via steam reforming. J Therm Anal Calorim. 2016;126(3):1621–31.
16. Li P. Thermodynamic analysis of waste heat recovery of molten blast furnace slag. Int J Hydrog Energy. 2017;42(15):9688–95.
17. Zuo ZL, Yu QB, Wei MQ, et al. Thermogravimetric study of the reduction of copper slag by biomass. J Therm Anal Calorim. 2016;126(2):481–91.
18. Warczok A, Riveros G. Slag cleaning in crossed electric and magnetic fields. Miner Eng. 2007;20(1):34–43.
19. Zuo ZL, Yu QB, Xie HQ, et al. Thermodynamic analysis of reduction in copper slag by biomass molding compound based on phase equilibrium calculating model. J Therm Anal Calorim. 2018;132(2):1277–89.